

An Experimental Study of the Electrode Fall Voltage in an MPD Thruster

IEPC-2007-115

*Presented at the 30th International Electric Propulsion Conference, Florence, Italy
September 17-20, 2007*

Daisuke Nakata*

University of Tokyo, 7-3-1, Hongo, Bunkyo-ku, Tokyo 113-8656, Japan

Kyoichiro Toki†

Tokyo University of Agriculture and Technology, 2-24-16, Nakacho, Koganei-shi, Tokyo 184-8588, Japan

Yukio Shimizu‡

Institute of Space and Astronautical Science, 3-1-1, Yoshinodai, Sagamihara-shi, Kanagawa 229-8510, Japan

Ikkoh Funaki§

Institute of Space and Astronautical Science, 3-1-1, Yoshinodai, Sagamihara-shi, Kanagawa 229-8510, Japan

Hitoshi Kuninaka¶

Institute of Space and Astronautical Science, 3-1-1, Yoshinodai, Sagamihara-shi, Kanagawa 229-8510, Japan

and

Yoshihiro Arakawa||

University of Tokyo, 7-3-1, Hongo, Bunkyo-ku, Tokyo 113-8656, Japan

Abstract: The upper limit of total electrode fall voltage was determined by using "zero-limit approximating method", which is one of the classical methods widely used in welding society. 5ch parallel electrode MPD was newly constructed and successfully operated in quasi-steady mode changing its electrode gap from 4mm to 1mm. It is considered that the intercept of the extrapolated line at the limit of $d=0$ mm indicates 18V as the upper limit of electrode fall. The electrode fall voltage was not drastically changed over the wide operational condition. Comparing with other's data, the validity of obtained value is discussed in this paper.

*Graduate Student, Department of Aeronautics and Astronautics, E-mail: nakata@ep.isas.jaxa.jp

†Professor, Department of Mechanical System Engineering, E-mail: toki@cc.tuat.ac.jp

‡Research Engineer, Space Transportation Division, E-mail: shimizu@isas.jaxa.jp

§Associate Professor, Space Transportation Division, E-mail: Funaki@isas.jaxa.jp

¶Professor, Space Transportation Division, E-mail: kuninaka@isas.jaxa.jp

||Professor, Department of Aeronautics and Astronautics, E-mail: arakawa@al.t.u-tokyo.ac.jp

Nomenclature

J	= discharge current (sum of 5 channel)
V	= total discharge voltage
V_a	= anode fall voltage
V_k	= cathode fall voltage
V_{arc}	= discharge voltage across bulk plasma (without anode and cathode fall)
V_t	= voltage drop due to the joule heating in bulk plasma
V_{EM}	= voltage drop due to the back EMF in bulk plasma
V_i	= voltage drop due to the ionization or dissociation of the propellant in bulk plasma
T	= thrust
T_e	= electron temperature
\dot{m}	= mass flow rate
u	= exhaust speed of the propellant
d	= electrode gap

I. Introduction

TO know the exact electrode fall is undoubtedly one of the biggest remaining problem in the field of MPD thruster. Now, a lot of advanced numerical simulation code has been developed but unknown sheath drop impede calculating the accurate voltage or efficiency. It is not so hard to adopt some sheath model into simulation but in each model, they typically requires a lot of unknown physical parameters; for example, to know the exact work function is not easy because it dreadfully depends on the surface condition or the temperature. The erosion rate due to the evaporation or the sputtering is also very ambiguous and intrinsic to each material or operational condition. Thus, it is quite difficult to know the sheath voltage from analytical model. Macroscopic view including experimental approach is desired to know the sheath voltage. Probe measurements are most typical way to know the rough value although some disturbance to the plasma is unavoidable. Gallimore measured anode fall voltage using this technique[1] and mentioned that the anode fall voltage was increased with J^2/\dot{m} and reached close to 50V when $J^2/\dot{m}=140\text{kA}^2\text{-s/g}$. Diamant[2] said that there is a transition point on the anode fall voltage. In the past literature, Clark[3] said that the typical cathode fall was 5V and anode fall was in the vicinity of 15V up to currents of 300kA. Saber[4] measured the heat flux into the anode using thermocouple equipped on the anode surface and estimated the anode fall voltage. In his result, anode fall was about 5V when $J^2/\dot{m}=10\text{kA}^2\text{-s/g}$. This way, sheath voltage can also be acquired by measuring anode heat flux.

There is another famous method to estimate the electrode fall. That is, the total arc voltage when the electrode gap is nearly zero is approximately regarded as the sum of anode and cathode fall voltage(V_a+V_k). This "zero-limit approximating method" has been widely used in welding society. Recently, Yokomizu[5] measured the fall voltage of argon arc using this method and reported that it was 16.5V in the case of Cu-W electrode at atmospheric pressure. Besides, it was almost constant regardless of discharge current up to 20kA. This method surely determines the upper limit of electrode fall voltage without any disturbance.

In most of studies using this method, facing rod-rod or rod-plate configuration was adopted and the experiment was carried out under atmospheric pressure. In the case of MPD thruster, the chamber pressure is lower than atmospheric pressure and kA class discharge current passes through both electrodes. Besides, the strong self-induced magnetic field is generated between both electrodes and the current paths are flown away into the exit of the channel. These effects (low pressure, kA class current and the existence of the magnetic field) cause the rack of the electrical career near the anode surface and spotty arc attachment and the voltage hash easily occur. Under such condition, it is unclear whether the electrode fall voltage increases or not.

In this study, an adequate setup was constructed to apply this "zero-limit approximating method" into typical condition of MPD thrusters and pointed out the upper limit of electrode fall voltage over wide range of J^2/\dot{m} . Obtained value will be useful to compensate the results of numerical analysis that does not include sheath voltage.

II. Experimental Apparatus

We newly constructed 5ch variable electrode gap MPD thruster (Fig.1,2). The reason to avoid typical cylindrical configuration and adopted rectangular thruster is that the strength of magnetic field cannot be kept constant in the case of cylindrical one when approaching both electrodes. The detail about this will be described later. Although we already have had 2-D MPD thruster and have reported a lot of experimental results [6][7], it was not adequate for the voltage fall measurement because it had too large electrode area to observe voltage hash phenomena. One of the voltage oscillation mechanism is often explained by the instability on the anode when the desired current exceeds beyond natural thermal electron flux into the anode[8]. This time, we carefully designed the 5ch variable electrode gap MPD thruster to be adequate for electrode fall measurement, reducing the anode area to about 30 % of existing cylindrical thruster[9] while the cathode area was not different (Table.1).

10 pieces of copper and 5 pieces of 2%ThO₂-W were manufactured as rectangular electrodes. As for the anode material, copper was always used but the cathode material can be switched. All the electrode pieces have the width of 6mm and the length of 45mm. Thin boron nitride plate was used as an insulator and it determines the accurate electrode gap. The accuracy of the thickness d was within 10 %.

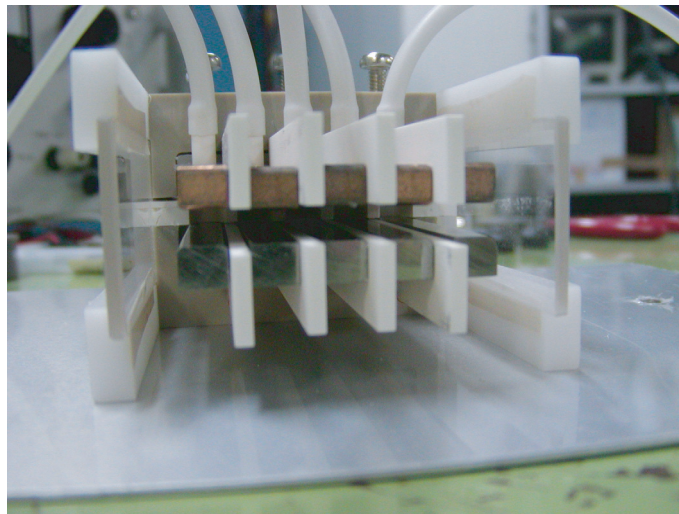


Figure 1. A front view of 5ch MPD ($d=4\text{mm}$).

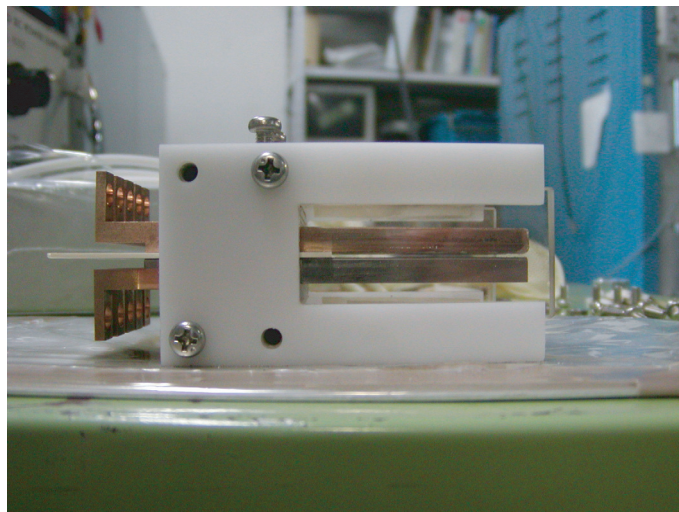


Figure 2. A side view of 5ch electrode MPD ($d=1\text{mm}$).

Table 1. The comparison of various MPD's electrode area.

Thruster	Anode area, cm ²	Cathode area, cm ²	Ref.
Cylindrical MPD ST-42	39.56	11.56	[9]
2-DMPD Straight	57.6	92.48	[6]
5ch variable electrode gap MPD	13.5	13.5	this paper

Although there are similar 5 parallel electrode pairs, we will focus on only the center channel (Ch.3) in the discussion. Figure.3 is a simulated magnetic field on the cross sectional plane at the channel inlet. Only in the intermediate region of Ch.3, the magnetic field is very uniform and close to the theoretically calculated value (assuming idealized infinite plane) while at both side channel (Ch.1 and Ch.5), the magnetic field is weakened and not uniform. This way, 5-channel structure was necessary to make idealized magnetic field even though only at the center channel. Each electrode was connected to 0.5 Ω resistors respectively and the channel-to-channel discharge characteristics was achieved.

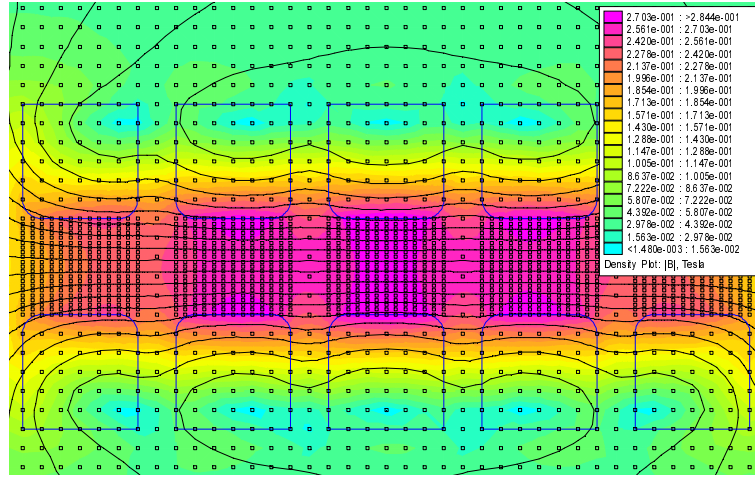


Figure 3. Calculated magnetic field (maximum strength of magnetic field 0.3T was achieved at the center channel.) of 5ch MPD at 10kA. (2kHz AC was assumed)

The thruster head was set in a stainless steel-vacuum tank of 0.8-m diam. and 2.0-m long, which was evacuated to less than 7mPa before each firing. 5-port fast acting valve (FAV) was used to supply 5-ms gas pulse. Working gas was introduced into discharge chamber through the root of each anode. After the gas was supplied enough in the whole discharge chamber, the ignitron of a pulse-forming network (PFN) was triggered. The PFN consists of 2mF-5kV capacitor bank and can supply 0.45ms flat-topped waveform of 20kA at maximum. Any ignition plug was not used in the discharge chamber. Each arc discharge was initiated by high voltage breakdown.

To perform voltage measurement, 5 sets of photo coupler and known resistors (8k Ω) were connected in parallel to each electrode. Generally the relation between the input voltage and photo coupler output showed nonlinear characteristics, so each one was calibrated carefully before the experiment. Considerable calibration error was below 0.3V at most. Two different data logger were used; the one enabled us 8ch data import while the sampling rate was not so high (Max. 100kHz). The other one has only 4ch data import but enabled high sampling rate (Max. 2GHz). The former one was used as coinstantaneous 5ch measurement and the latter was used when we only focused on the characteristics of the center electrode (Ch.3).

The mass shot of each firing was determined by the pressure reduction of second reserver tank. Since we adopted very small mass flow rate (0.2g/s) in this experiment, considerable error was not small (< 20 %).

III. Experimental Results

First, the discharge voltage waveforms of 5 channels measured simultaneously are shown in Fig.4-Fig.7 (Red=Ch.1, Yellow=Ch.2, Green=Ch.3 Light Blue=Ch.4 Blue=Ch.5). When the discharge current is small, each channel showed almost same voltages but as the discharge current becomes larger, generally Ch.1 and Ch.5 showed higher voltages than the others. This would be caused by the nonuniformity of the magnetic field mentioned in Fig 3, that is, it was supposed that the current path lean to edge side. As for the discharge current, although it was not confirmed, the uniformity will be achieved by the existence of 500m Ω resistor connected to each channel. Total discharge current was measured at the PFN by using Rogowski coil.

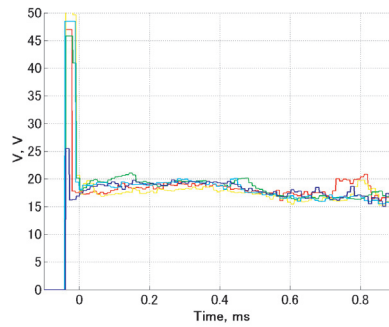


Figure 4. Discharge voltage waveform of 5ch MPD at $J=2.1\text{kA}$, $d=1\text{mm}$. The sampling rate was 100kHz.

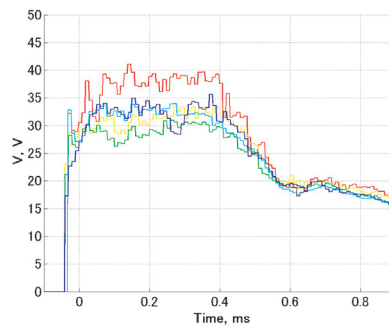


Figure 5. Discharge voltage waveform of 5ch MPD at $J=10.8\text{kA}$, $d=1\text{mm}$. The sampling rate was 100kHz.

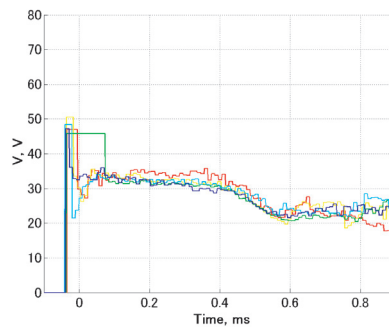


Figure 6. Discharge voltage waveform of 5ch MPD at $J=2.1\text{kA}$, $d=4\text{mm}$. The sampling rate was 100kHz.

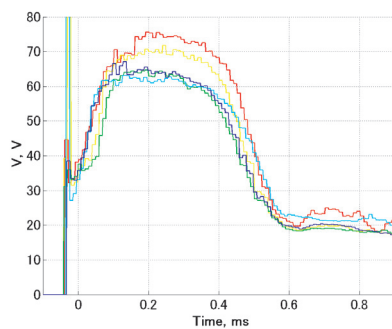


Figure 7. Discharge voltage waveform of 5ch MPD at $J=10.8\text{kA}$, $d=4\text{mm}$. The sampling rate was 100kHz.

Now focusing on Ch.3, which has the most stable self-induced magnetic field, the discharge current vs. discharge current characteristics when changing the electrode gap is shown in Fig.8. 5 data points were acquired for a fixed operational condition. Some sort of knee point is recognized and a certain amount of voltage hash was recognized at above 9kA for each electrode gap, especially in the case of $d=3$ or 4mm.. As an example of voltage hash, several voltage waveforms of Ch.3 are presented in Fig.9-Fig.12. It is supposed that the rack of electron near the anode caused such oscillations. (See in Ref.[9] or[10])

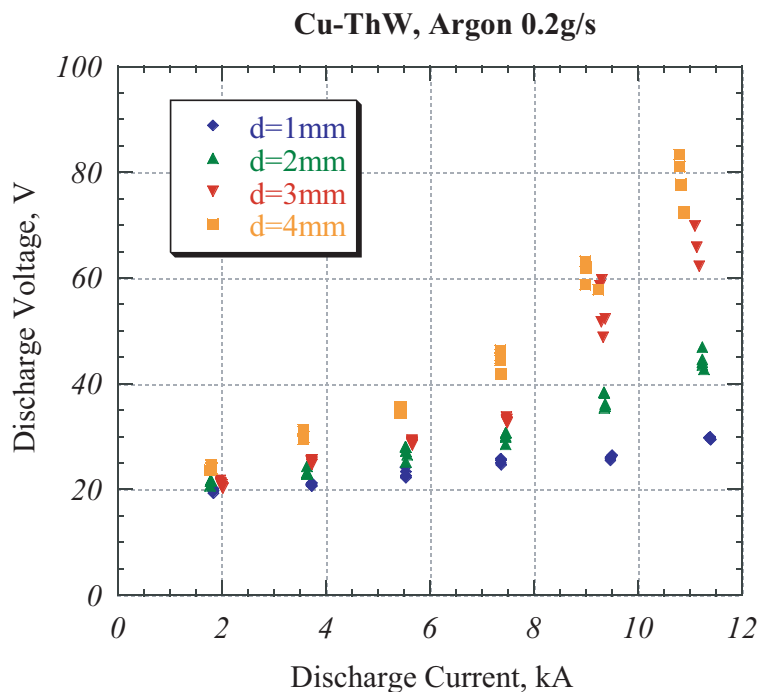


Figure 8. Voltage characteristics against discharge current

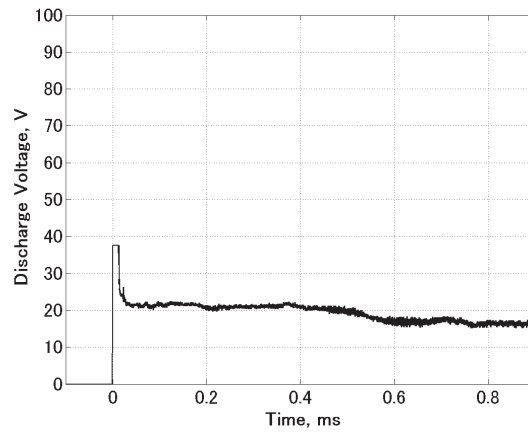


Figure 9. Discharge voltage waveform of Ch.3 at $J=3.6\text{kA}$, $d=1\text{mm}$. The sampling rate was 10MHz.

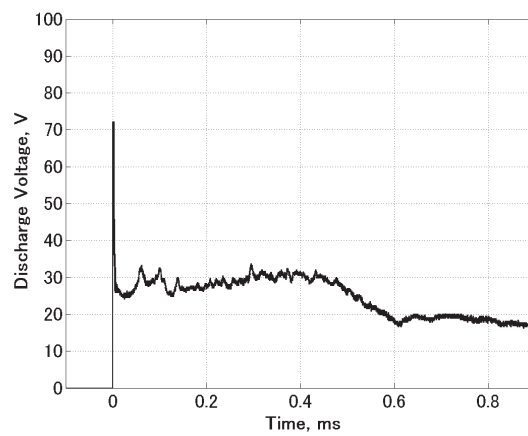


Figure 10. Discharge voltage waveform of Ch.3 at $J=10.8\text{kA}$, $d=1\text{mm}$. The sampling rate was 10MHz.

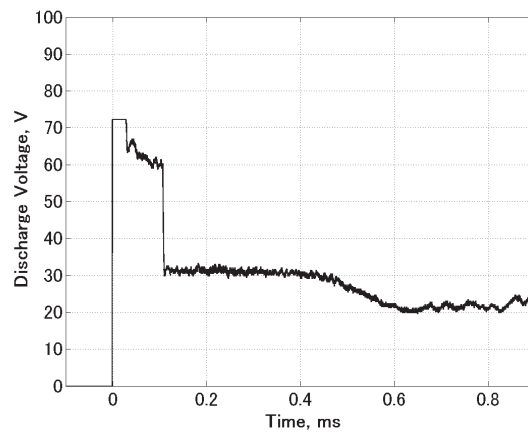


Figure 11. Discharge voltage waveform of Ch.3 at $J=3.6\text{kA}$, $d=4\text{mm}$. The sampling rate was 10MHz.

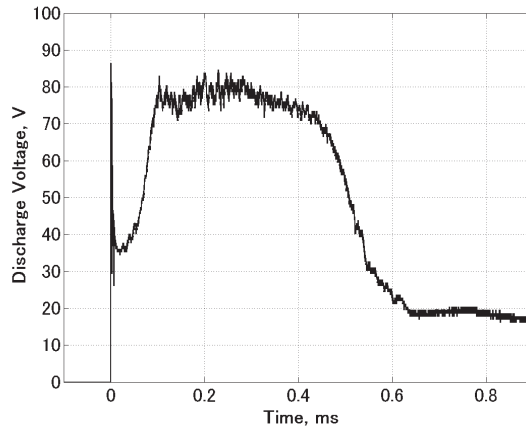


Figure 12. Discharge voltage waveform of Ch.3 at $J=10.8\text{kA}$, $d=4\text{mm}$. The sampling rate was 10MHz.

In Fig.13 the voltage characteristics against electrode gap at 2.1, 3.6, 5.5, 7.4, 9.1, and 10.8kA are plotted and linearized lines are also presented. The intercepts of these lines are supposed to be the total sheath drop ($V_a + V_k$). In the case of 2.1, 3.6, 5.5 and 7.4kA, the approximated lines are similarly approaching into 18V. As for the cases of 9.1 and 10.8kA, the intercepts of the extrapolated lines are below 15V. These cases are within the range of "voltage hash region" and severe electrode erosion was recognized on the anode surface. Drastically eroded region was on the tip of the electrode (Fig.14-15) and sometimes the discharge current was attached on the outer surface of the anode. It was easily considered that the discharge current paths become longer than its electrode gap length d in the case of 9.1 and 10.8kA. Therefore, the plotted points might have to be shifted into the forward direction (see Fig.16). This point will be discussed later again.

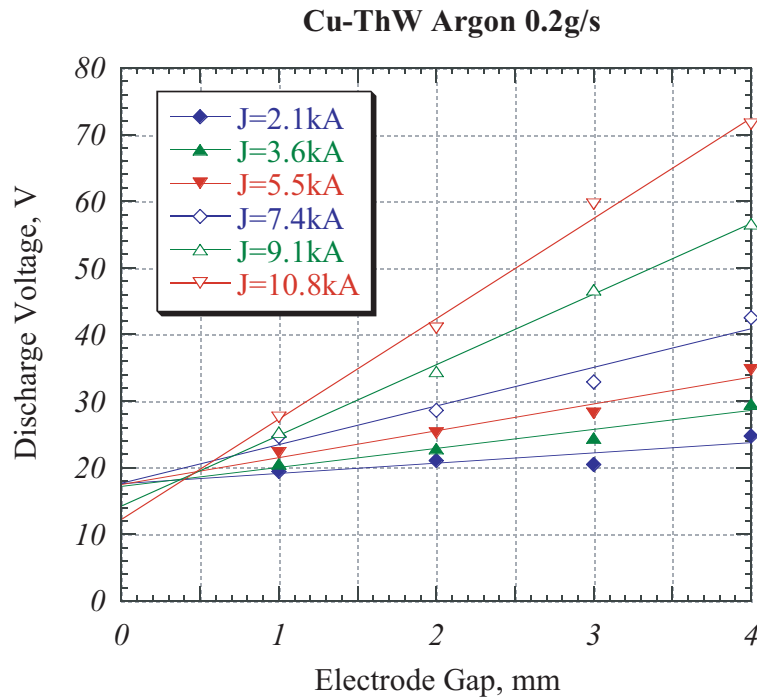


Figure 13. Voltage characteristics against electrode gap.

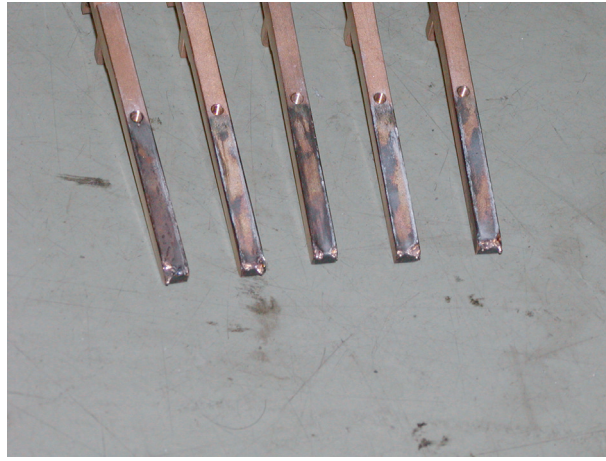


Figure 14. Anode surface after intense firing.

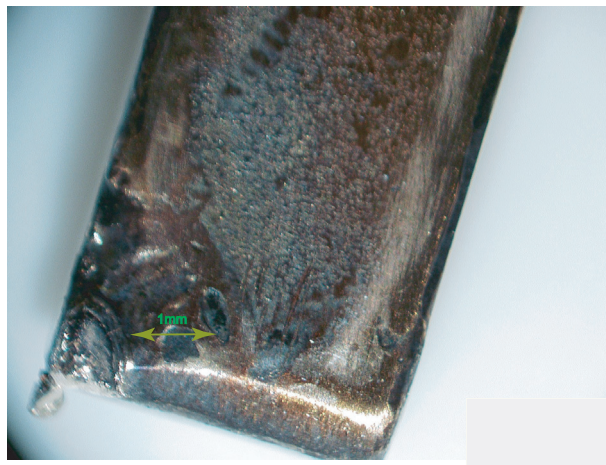


Figure 15. Melted anode tip.

IV. Discussion

A. The validity of the "zero-limit approximating method"

This method has long been used in welding society[11-15] and there is a lot of reported values of electrode fall. Moreover, the critical points to yield misunderstandings have been also mentioned in some literatures[11]. The electron temperature is quite important parameter although it was not measured in this study. Peuckert and Finkelburg[12] experimentally showed that the anode fall voltage was very sensitive to the electron temperature in front of the anode surface. $V_a=4V$ was reported when $T_e=16000K$, whereas $V_a=1V$ was reported when $T_e=20000K$ [12]. Besides, it was also reported that the electron temperature tended to become higher as reducing electrode gap even if the other condition was completely same.

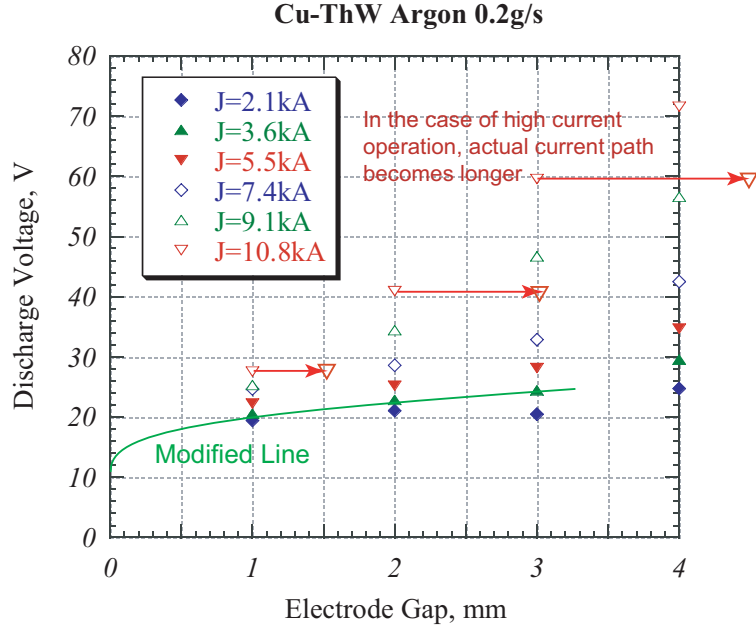


Figure 16. Modified voltage characteristics against electrode gap based on some considerable errors.

Second, there is a problem how long the actual arc length is. Even in the case of facing rod to rod configuration, the arc column was flown off and the actual arc path often became about 1-1.5 times longer than the electrode gap length d . In addition to this, in the case of this experiment, it is unavoidable that the current path is flown off by Lorenz force. However, if the tilt angle of each case (when changing electrode gap at a fixed discharge current) is same, in other words, if actual current path is similarly proportional to d , the intercept will not change. Therefore, in the case of relatively small J , this method works well. On the other hand, the current path is blown off far away from the anode tip in the case of very high discharge current. In such a case, the validity of this method will become uncertain. Actual current path can be measured by magnetic probe or magnetic sensitive film[7] and some modification should be applied to d .

One may think the potential gradient may not be constant and the linearized approximation in Fig.13 is not accurate. Actually, the potential gradient near the electrode may not be constant, it is reported that the potential gradient becomes gradually steep [13][14] within 1mm from the electrode wall (as like as the green line in Fig.16). But at least, it is considered that the total electrode fall will not exceed the discharge voltage V at $d=1\text{mm}$ and the error can be reduced if we obtained the data at much closer point (ex. 0.5mm or 0.3mm). Now, in order to obtain more precise understandings, we estimate the conceivable voltage drop across bulk plasma.

The potential drop between both electrodes will be roughly described as the sum of $V_a + V_k + V_{EM} + V_t + V_i$ [16]. $V_a + V_k$ corresponds the total sheath drop and the other is considered as the voltage drop across bulk plasma. In the case of our 5ch MPD, the electromagnetic thrust can be calculated theoretically[17] by following equation. W is a electrode width and only blowing force was considered.

$$T_{EM} = \frac{\mu_0 J^2}{8} \left(\frac{d}{W} \right) \quad (1)$$

Substituting $W=30\text{mm}$, we obtained $T(N) = 5.23 * 10^{-3} d(\text{mm}) J^2(\text{kA})$. This is very small compared to the cylindrical MPD thruster[9]. For example, $T=2.1\text{N}$ in the case of $J=10\text{kA}$ and $d=4\text{mm}$. V_{EM} can be described as follows;

$$JV_{EM} = \frac{1}{2} \dot{m} u^2 \quad (2)$$

$$V_{EM} = \frac{T^2}{2\dot{m}J} = \frac{\mu_0^2 J^3}{128\dot{m}} \left(\frac{d}{W} \right)^2 \quad (3)$$

Substituting W and $\dot{m}=0.2\text{g/s}$, considerable V_{EM} is only 1.1V even in the case of $J = 10\text{kA}$ and $d = 4\text{mm}$. Thus, the electro magnetic force and its back EMF is found to be quite small in 5ch MPD. Next, V_t is considered to be proportional to the arc length as long as the conductivity is constant. In the case of welding arc or the case of the constrictor arc of DC arcjets, this assumption is adopted. Since V_{EM} was found to be very small, it can be said that most of voltage drop across bulk plasma will be dominated by V_t .

As for the value of V_i , it had been considered[18] that; V_i is already included in V_k so that the electrons accelerated in the cathode fall region effectively ionize the neutrals. According to this assumption, V_k must be larger than the first ionization potential of the working gas but from several experiments, it was found that such a high voltage fall are not necessary; for example, It was reported that the TIG arc using argon as a working gas was successfully operated at 7.5V of total discharge voltage, which is clearly below than the ionization voltage of argon. Today, the value V_k is supposed to be between the ionization potential of the working gas and that of the cathode material. This idea implies that the evaporated cathode material strongly affects the ionization process of the working gas. If the thermal ionization dominates the most of ionization process, as this is quite possible assumption in the case of MPD thruster, V_i will be included as a part of V_t . Therefore, the authors think it is not necessary to separate V_i from V_k or V_t .

Returning to Fig.8, we reconsider the difference between the total discharge voltage and the electrode fall $V_a + V_k$. As mentioned before, V_{EM} is almost negligible. So the most of difference is caused by V_t , similarly in the case of welding arc.

The components that will affect the determination of electrode fall voltage and considerable way to solve them are summarized as follows;

- There is the possibility the electron temperature in front of the electrode surface is increased as reducing the electrode gap. The differences of T_e must be cleared beforehand.
- Typically the potential gradient tends to be steep near the electrode. Acquiring the data at closer point solves the problem.
- There is no effect for the intercept of the approximated line if the current path is similarly tilted by Lorenz force, but in case that the the current path is strongly blown off from electrode, the actual current path must be measured and the value of d should be modified.

B. Anode fall behavior under the voltage hash condition

Whether the drastic increase of the anode fall voltage occurs or not under voltage hash condition is one of the significant problem.

Diamant[2] reported that the sudden increase of anode fall voltage when the parameter ξ defined as follows exceed 1. (See [2] or [20] about the detail meanings of the parameter ξ .)

$$\xi = \left(\frac{\mu_0 J^2 \ln(r_a/r_c)}{4\pi\dot{m} \ 2\varepsilon_i/M} \right)^{1/2} \quad (4)$$

He explained this was related to spot mode arc attachment on the anode. In our study, however, any drastic increase of total electrode fall was recognized while melting anode was surely observed above 9kA (Fig.15).

Threshold of instability was defined by several parameters. Most famous one is J^2/\dot{m} used to consider Alfvén onset condition. In this experiment, J^2/\dot{m} was varied from 22(1.8kA) to 583(10.8kA) $\text{kA}^2\text{-s/g}$. Another way to determine the threshold current is based on the starvation of electron near the anode. the electron flux at a certain point into the anode is considered as follows,

$$\Gamma_e = \frac{n_e}{4} \left(\frac{8eT_e}{\pi m_e} \right) \quad (5)$$

And when J_{th} defined as below exceeds the current desired by external circuit, anode spot transition will occur[8].

$$J_{th} = \int_S e\Gamma_e dA_{anode} \quad (6)$$

According to this assumption, the threshold current is about 5kA in this 5ch MPD if $n_e=10^{20}\text{m}^{-3}$ and $T_e=2\text{eV}$ were assumed. Of course, local distribution of n_e and T_e is absolutely necessary in accurate calculation. We will try to determine the values of n_e and T_e along the electrode using spectroscopic measurement hereafter.

Uribarri[8] calculated the order of the oscillation under the voltage hash mode and the result was a few MHz order.

In this experiment, we analyzed FFT spectrum under the voltage hash condition(Fig.17, 18). Indeed, it seems that MHz order spectrum becomes stronger in the case of 10.8kA, but more precise discussion using a lot of number of experimental data will be needed. Besides, direct spot observation using high-speed camera or high speed radiation thermometer is currently planned.

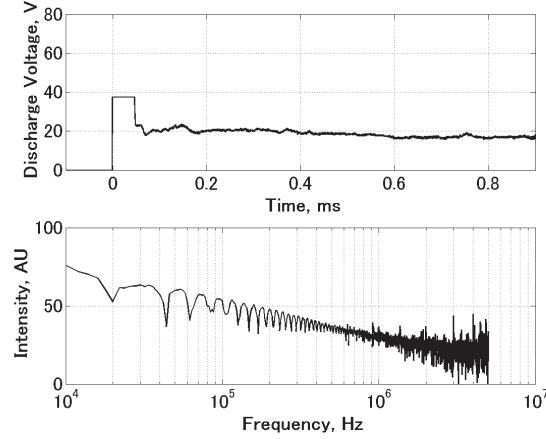


Figure 17. Voltage waveform and FFT spectrum of Ch.3 at $J=2.1\text{kA}$, $d=1\text{mm}$. The sampling rate was 10MHz.

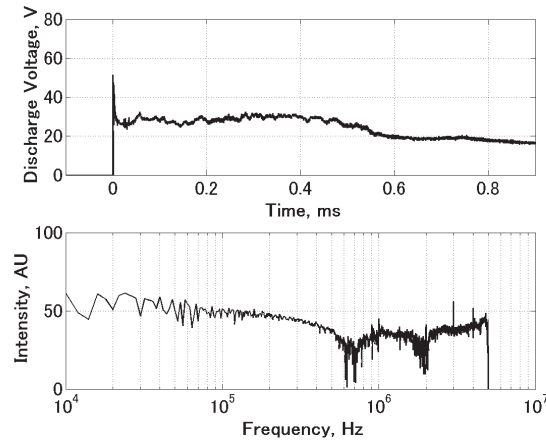


Figure 18. Voltage waveform and FFT spectrum of Ch.3 at $J=10.8\text{kA}$, $d=1\text{mm}$. The sampling rate was 10MHz.

V. Conclusion

The exact value of electrode fall voltage in an MPD thruster is strenuously desired by researchers in the field of numerical simulation. In this study, we applied "zero-limit approximation method", which has been widely accepted in welding society to determine total electrode fall, into MPD condition (arranging pressure, current density on the electrode surface, and so on) and obtained following results.

- 5ch variable electrode gap MPD thruster was newly constructed and successfully operated. Some kind of threshold of voltage hash was recognized above $J = 9\text{kA}$ and $\dot{m} = 0.2 \text{ g/s}$ in the case of Argon.

- Determined total electrode fall voltage (V_a+V_k) was supposed to be 18 V as a result of "zero limit approximating method" changing electrode gap from 4mm to 1mm. At least, it is considered that the true value should be below 20V, which is the total discharge voltage in the case of 1mm electrode gap.
- Above 9kA, the anode was drastically eroded and the voltage hash was observed. However, it was considered that the total electrode fall voltage was not so increased even in such condition.
- It is necessary to solve considerable uncertainty in this study. First, the electron temperature near the electrode surface must be measured in each case. Second, the actual current path has to be examined using magnetic probe. If the spotty arc attachment was observed using high-speed camera, it will be informative to specify the mode transition.

Acknowledgments

This work was supported by a Grant-in-Aid for JSPS(Japan Society for Promotion of Science). The author was supported through the 21st Century COE Program, " Mechanical Systems Innovation " by the Ministry of Education, Culture, Sports, Science and Technology in Japan.

References

- ¹A., D., Gallimore, A., J., Kelly and R., G., Jahn, "Anode Power Deposition in Magnetoplasmadynamic Thrusters," *Journal of Propulsion and Power*, Vol. 9, No. 3, 1993, pp. 361-368.
- ²K., D., Diamant, E., Y., Choueiri and R., G., Jahn, "Spot Mode Transition and the Anode Fall of Pulsed Magnetoplasmadynamic Thrusters," *Journal of Propulsion and Power*, Vol. 14, No. 6, 1998, pp. 1036-1042
- ³Kenn E., Clark, "Quasi-Steady Plasma Acceleration," *AIAA Journal*, Vol. 8, No. 2, 1970, pp. 216-220.
- ⁴A., J., Saber and R., G., Jahn, "Anode Power in Quasisteady Magnetoplasmadynamic Accelerators," *AIAA Journal*, Vol. 16, No. 4, 1978, pp. 328-333.
- ⁵Y., Yokomizu, T., Matsumura, R., Henmi and Y., Kito, "Total voltage drops in electrode fall regions of SF6, argon and air arcs in current range from 10 to 20000A," *J. Phys. D: Appl. Phys.*, Vol. 29, 1996, pp. 1260-1267.
- ⁶K., Toki, M., Sumida and K., Kuriki, "Multichannel Two-Dimensional Magnetoplasmadynamic Arcjet," *Journal of Propulsion and Power*, Vol. 8, No. 1, 1992, pp. 93-97.
- ⁷I., Funaki, K., Toki, and K., Kuriki, "Electrode Configuration Effect on the Performance of a Two-Dimensional Magnetoplasmadynamic Arcjet," *Journal of Propulsion and Power*, Vol. 14, No. 6, 1998, pp. 361-368.
- ⁸L., Uribarri and E., Y., Choueiri, "The Onset of Voltage Hash and its Relationship to Anode Spots in Magnetoplasmadynamic Thrusters," IEPC Paper 2005-084, 2005.
- ⁹D., Nakata, K., Toki, I., Funaki, Y., Shimizu, H., Kuninaka and Y., Arakawa, "Recent Study for Electrode Configuration and Material Improvement in an MPD Thruster," AIAA Paper 2007-5279, Jul., 2007.
- ¹⁰K., Kuriki and H., Iida, "Spectrum Analysis of Instabilities in MPD Arcjet," IEPC 84-28, 1984.
- ¹¹Lancaster, J., F., *The Physics of Welding*, 2nd ed., The International Institute of Welding, 1986, Chaps. 6.
- ¹²Busz-Peuckert, G., Finkelnburg, W., "Die Abhängigkeit des Anodenfalls von Stromstärke und Bogenlänge bei Hochtemperaturbögen," *Z. Phys.*, Vol. 140, 1955, pp. 540.
- ¹³Lancaster, J., F., "Energy Distribution in argon-shielded welding arcs," *Brit. Weld. J.*, Vol. 1, 1954, pp. 412-426.
- ¹⁴Jackson, C., E., "The Science of Arc Welding," *Weld. J.*, Vol. 39, 1960, pp. 129s-140s, 177s-190s, 225s-230s.
- ¹⁵Davis., E., and Terry., C., A., "Nitrogen-Arc Welding with Copper," *Brit. Weld. J.*, Vol. 1, 1954, pp. 53.
- ¹⁶D., Nakata, "Experimental Approach to the Optimization of MPD Electrode Geometry," IAC-04-S.4.05, Oct., 2004.
- ¹⁷Kyoichi Kuriki and Hiroshi Suzuki, "Transitional Behavior of MPD Arcjet Operation," *AIAA Journal.*, Vol. 16, No.10, 1978, pp. 62s-67s.

¹⁸Spraragen, W., and Lengyel, B., A., "Physics of the arc," *Weld. J.*, Vol. 22, 1943, pp. 2s-42s.

¹⁹Busz-Peuckert, G., Finkelnburg, W., "*Thermische Lichtbögen* hoher Temperatur und niedriger Brennspannung," *Z. Phys.*, Vol. 139, 1954, pp. 212.

²⁰E.Y., Choueiri, A., J., Kelly and R., G., Jahn, "MPD Thruster Plasma Instability Studies," AIAA Paper 87-1067, May, 1987.